

# Exclusive pseudoscalar and heavy vector mesons production using GPD approach in EIC

Ya-Ping Xie

Institute of Modern Physics, CAS

Collaborated with S. V. Goloskokov and V. Goncalves

Based on arXiv: 2408.05800, 2502.17743 and 2507.20448

Apr 22, 2026

# Outline

This slide focus on the gluon GPDs to study vector meson production. It contains follow sections:

- Introduction to GPDs
- Process in ep scattering to study GPDs
- Time like Compton Scattering using GPD in EIC
- Pseudoscalar meson production using GPD in EIC
- Vector meson production within GPD in EIC
- Summary

# Introduction to GPDs

Generalized Parton Distributions (GPDs) can be extracted from Deep Virtual Compton Scattering ( DVCS), Double Deep Virtual Compton Scattering(DDVCS) Time-like Compton Scattering (TCS) and Hard Exclusive Meson Production (HEMP) processes. GPDs can be employed to study

- Spin puzzle
- Energy Momentum tensor
- Gravitational form factor
- Mass radius, distributions and pressure

## Sum rules of GPDs

There are several kinds of GPD function,  $H_q, E_q, \tilde{H}_q, \tilde{E}_q$ . There are similar for gluon GPDs.

GPD connects parton distribution via  $H(x, 0, 0) = xf(x)$ . Hadron Form factor can be obtain from GPDs

$$\int dx H^q(x, \xi, t) = F_1^q(t), \quad \int dx E_q(x, \xi, t) = F_2^q(t); \quad (1)$$

$$\int dx \tilde{H}^q(x, \xi, t) = G_A^q(t), \quad \int dx \tilde{E}^q(x, \xi, t) = G_p^q(t). \quad (2)$$

Ji sum rules for the proton angular memonta

$$\int x dx (H^q(x, \xi, 0) + E^q(x, \xi, 0)) = 2J^q. \quad (3)$$

- GPDs  $H^q$  and  $E^q$  can be tested in  $\rho$  meson production
- $\tilde{H}^q$  and  $\tilde{E}^q$  can be tested in  $\pi^0$  production

## Quark helicity conservation distributions

The quark helicity conservation distributions go with the Dirac matrix  $\gamma^+$  and  $\gamma^+ \gamma_5$ , where  $i = 1, 2$  is a transverse index, it is defined as [EPJC-19-485]

$$\begin{aligned} & \frac{1}{2} \int \frac{dz^-}{2\pi} e^{ixP^+z^-} \langle p', \lambda' | \bar{\psi}(-\frac{1}{2}z) \gamma^+ \psi(\frac{1}{2}z) | P, \lambda \rangle |_{z^+=0, z_T=0} \\ &= \frac{1}{2P^+} \bar{u}(p', \lambda') \left[ H^q \gamma^+ + E^q \frac{i\sigma^{+\alpha} \Delta_\alpha}{2m} \right] u(p, \lambda). \end{aligned} \quad (4)$$

$$\begin{aligned} & \frac{1}{2} \int \frac{dz^-}{2\pi} e^{ixP^+z^-} \langle p', \lambda' | \bar{\psi}(-\frac{1}{2}z) \gamma^+ \gamma_5 \psi(\frac{1}{2}z) | P, \lambda \rangle |_{z^+=0, z_T=0} \\ &= \frac{1}{2P^+} \bar{u}(p', \lambda') \left[ \tilde{H}^q \gamma^+ \gamma_5 + \tilde{E}^q \frac{\gamma_5 \Delta^+}{2m} \right] u(p, \lambda). \end{aligned} \quad (5)$$

$H^q$ ,  $E^q$ ,  $\tilde{H}^q$  and  $\tilde{E}^q$  are quark helicity conservation distributions.

# Gluon GPD

The gluon GPD have four parts of GPDs

$$\begin{aligned} & \langle p'v' | \sum_{a,a'} A^{a\rho}(0) A^{a'\rho'}(\bar{z}) | pV \rangle \\ &= \frac{1}{2} \sum_{\lambda=\pm 1} \varepsilon^\rho(k_g, \lambda) \varepsilon^{*\rho'}(k_g, \lambda') \quad (6) \\ & \times \int_0^1 \frac{dx}{(x+\xi-i\varepsilon)(x-\xi+i\varepsilon)} e^{-i(x-\xi)p\cdot\bar{z}} \\ & \times \left\{ \frac{\bar{u}(p'v') \not{n} u(pV)}{2\bar{p}\cdot n} H^g(x, \xi, t) + \frac{\bar{u}(p'v') i \sigma^{\alpha\beta} n_\alpha \Delta_\beta u(pV)}{4m \bar{p}\cdot n} E^g(x, \xi, t) \right. \\ & \left. + \lambda \frac{\bar{u}(p'v') \not{n} \gamma_5 u(pV)}{2\bar{p}\cdot n} \tilde{H}^g(x, \xi, t) + \lambda \frac{\bar{u}(p'v') n \cdot \Delta \gamma_5 u(pV)}{4m \bar{p}\cdot n} \tilde{E}^g(x, \xi, t) \right\}. \end{aligned}$$

## Quark helicity flip distributions

The quark helicity flip distributions go with the Dirac matrix  $\sigma^{+i}$ , where  $i = 1, 2$  is a transverse index, it is defined as[EPJC-19-485]

$$\begin{aligned} & \frac{1}{2} \int \frac{dz^-}{2\pi} e^{ixP^+z^-} \langle p', \lambda' | \bar{\psi}(-\frac{1}{2}z) i\sigma^{+i} \psi(\frac{1}{2}z) | P, \lambda \rangle |_{z^+=0, z_T=0} \\ &= \frac{1}{2P^+} \bar{u}(p', \lambda') \left[ H_T^q i\sigma^{+i} + \tilde{H}_T^q \frac{P^+ \Delta^i - \Delta^+ P^i}{m^2} \right. \\ & \left. + E_T^q \frac{\gamma^+ \Delta^i - \Delta^+ \gamma^i}{2m} + \tilde{E}_T^q \frac{\gamma^+ P^i - P^+ \gamma^i}{m} \right] u(p, \lambda). \end{aligned} \quad (7)$$

$H_T^q$ ,  $\tilde{H}_T^q$ ,  $E_T^q$  and  $\tilde{E}_T^q$  are quark helicity flip distributions.

# Physical processes to study GPD

There are several processes can be studied GPDs in ep scattering

- Deep Virtual Compton Scattering (DVCS)
- Time-like Compton Scattering (TCS)
- Double Deep Virtual Compton Scattering (DDVCS)
- Deep Virtual Meson Production (DVMP)

# Deep Virtual Compton Scattering

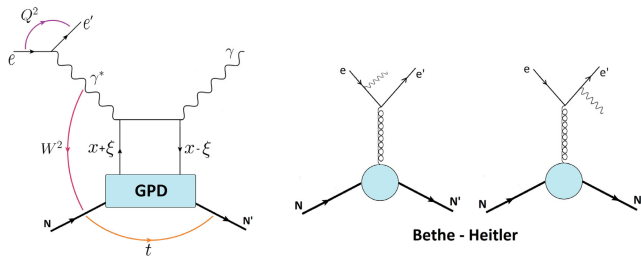


Figure 1: DVCS schematic diagram.

# Double Deep Virtual Compton Scattering

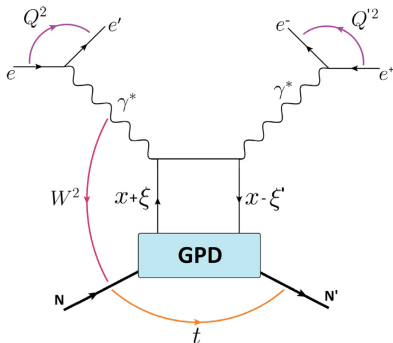


Figure 2: DDVCS schematic diagram.

# Time Compton Scattering

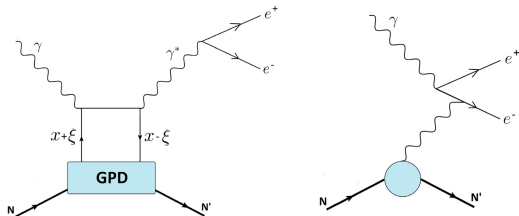


Figure 3: TCS schematic diagram.

In TCS, the differential cross section are given as [EPJC-23-675]

$$\frac{d\sigma_{\gamma p \rightarrow l+l^-p}^{TCS}}{dQ^2 dt d(\cos\theta) d\phi} = \frac{\alpha_{em}^3}{8\pi s_{\gamma p}^2} \frac{1}{Q^2} \frac{1+\cos^2\theta}{2} \left\{ (1-\eta^2)(|\mathcal{H}_1|^2 + |\widetilde{\mathcal{H}}_1|^2) - 2\eta^2 \text{Re}(\mathcal{H}_1^* \widetilde{\mathcal{E}}_1) - \eta^2 \frac{t}{4M_p^2} |\widetilde{\mathcal{E}}_1|^2 \right\}, \quad (8)$$

$$\begin{aligned} \frac{d\sigma_{\gamma p \rightarrow l+l^-p}^{INT}}{dQ^2 dt d(\cos\theta) d\phi} &= -\frac{\alpha_{em}^3}{4\pi s_{\gamma p}^2} \frac{\sqrt{t_0-t}}{-tQ} \frac{\sqrt{1-\eta}}{\eta} \left( \cos\phi \frac{1+\cos^2\theta}{\sin\theta} \right) \\ &\times \text{Re} \left[ F_1(t) \mathcal{H}_1 - \eta(F_1(t) + F_2(t)) \widetilde{\mathcal{H}}_1 - \frac{t}{4M_p^2} F_2(t) \mathcal{E}_1 \right], \end{aligned} \quad (9)$$

# TCS cross section

The differential cross section of TCS at p-Pb UPC using GK model [arXiv.2212.07657].

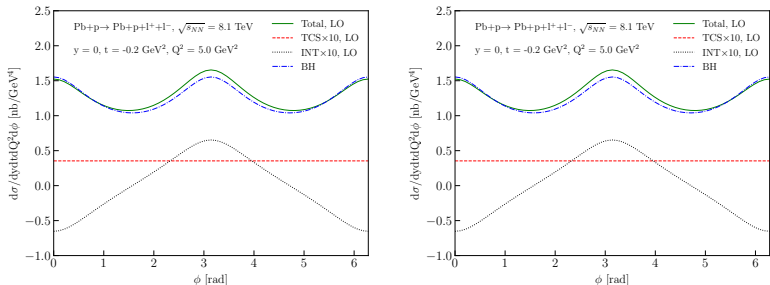


**Figure 4:** Azimuthal distributions of the lepton pair for fixed values of  $Q^2$  and  $t$  and two values of rapidity considering ultraperipheral pPb collisions at  $\sqrt{s_N}N = 8.1$  TeV..



## PM production

In the process  $\gamma^* + p \rightarrow \pi + p$  [EPJC-65-137]

$$\frac{d^2\sigma}{dt d\phi} = \frac{1}{2\pi} \left( \frac{d\sigma_T}{dt} + \varepsilon \frac{d\sigma_L}{dt} + \varepsilon \cos 2\phi \frac{d\sigma_{TT}}{dt} + \sqrt{2\varepsilon(1+\varepsilon)} \cos \phi \frac{d\sigma_{LT}}{dt} \right) \quad (10)$$

For Pseudoscalar meson production. The cross section can be expressed as

$$\frac{d\sigma_L}{dt} = \frac{4\pi\alpha}{k'Q^6} \left[ (1 - \xi^2) |\langle \tilde{H} \rangle|^2 - 2\xi^2 \text{Re}[\langle \tilde{H} \rangle^* \langle \tilde{E} \rangle] - \frac{t'}{4m^2} \xi^2 |\langle \tilde{E} \rangle|^2 \right], \quad (11)$$

$$\frac{d\sigma_T}{dt} = \frac{4\pi\alpha\mu_\pi^2}{2k'Q^8} \left[ (1 - \xi^2) |\langle H_T \rangle|^2 - \frac{t'}{8m^2} |\langle \tilde{E}_T \rangle|^2 \right], \quad (12)$$

$$\frac{d\sigma_{LT}}{dt} = \frac{4\pi\alpha\mu_\pi}{\sqrt{2}k'Q^7} \frac{\sqrt{t'}}{2m} \xi \sqrt{1 - \xi^2} \text{Re}[\langle H_T \rangle^* \langle \tilde{E} \rangle], \quad (13)$$

$$\frac{d\sigma_{TT}}{dt} = \frac{4\pi\alpha\mu_\pi^2}{2k'Q^8} \frac{t'}{16m^2} |\langle \tilde{E}_T \rangle|^2. \quad (14)$$

## PM scattering amplitude

For twist-2 convolution function is given as

$$\mathcal{H}_{0\lambda,0\lambda}^{\text{twist-2}} = 4\pi\alpha_s(\mu_R) \int dz d^2\mathbf{k}_\perp \Psi_\pi^{(2)}(z, \mathbf{k}_\perp) \mathcal{F}^{(2)}(z, x, \xi, \mathbf{k}_\perp). \quad (15)$$

The hard subprocess of twist-2 is written as

$$\mathcal{F}^{(2)}(z, x, \xi, \mathbf{k}_\perp) = C_F \sqrt{\frac{2}{N_c}} \frac{Q^2}{\xi} (T_s - T_u). \quad (16)$$

$T_s$  and  $T_u$  are propagator which are defined as

$$T_s = \frac{1}{\bar{z}Q^2(x - \xi)/(2\xi) - \mathbf{k}_\perp^2 + i\epsilon}. \quad (17)$$

$$T_u = \frac{1}{-zQ^2(x + \xi)/(2\xi) - \mathbf{k}_\perp^2 + i\epsilon}. \quad (18)$$

# PM scattering amplitude

The twist-3 convolution function is defined as

$$\begin{aligned} \mathcal{H}_{0-++}^{twist-3} &= \frac{2}{\pi^2} \frac{C_F}{\sqrt{2N_C}} \int dz d^2\mathbf{k}_\perp \Psi_{\pi P}^{(3)}(z, \mathbf{k}_\perp) \alpha_s(\mu_R) \\ &\times \left[ \frac{1}{x - \xi + \varepsilon} \frac{1}{\bar{z} \frac{x - \xi}{2\xi} Q^2 - \mathbf{k}_\perp^2 + \varepsilon} - \frac{1}{x + \xi + \varepsilon} \frac{1}{-z \frac{x + \xi}{2\xi} Q^2 - \mathbf{k}_\perp^2 + \varepsilon} \right] \quad (19) \end{aligned}$$

# $\pi^0$ cross section

The  $\pi^0$  cross section at CLAS are shown as [arXiv.2206.06547]

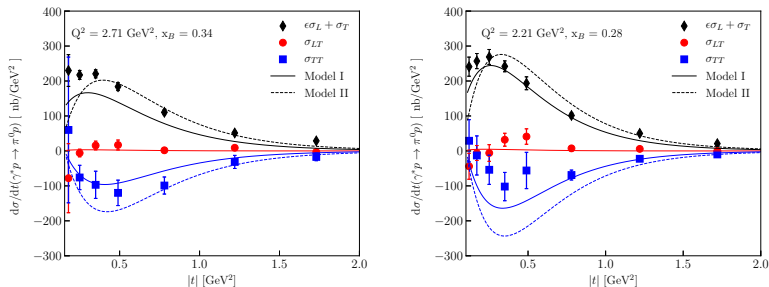


Figure 6: Cross section of  $\pi^0$  production in the CLAS energy range together with the CLAS data. Black lines are  $\sigma = \sigma_T + \epsilon\sigma_L$ , red lines label  $\sigma_{LT}$ , and blue lines present  $\sigma_{TT}$ .

# $\pi^0$ cross section

The  $\pi^0$  cross section at EicC are shown as [arXiv.2206.06547]

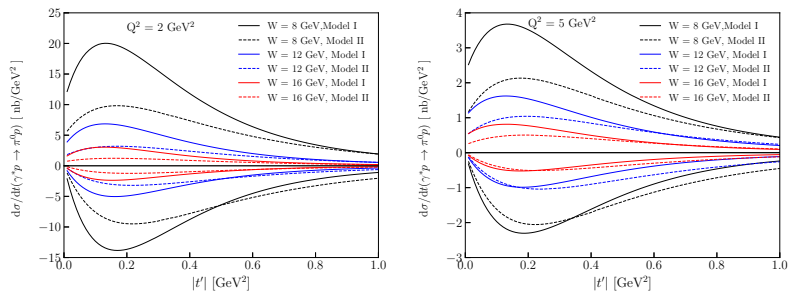


Figure 7: Models results for  $\sigma$  and  $\sigma_{TT}$  cross section at EicC kinematics.  $W$  dependencies at fixed  $Q^2$  are shown

# Vector meson production

GPDs can be employed to study meson production in several process.

- $\rho$  production ( $\frac{2}{3}H^u + \frac{1}{3}H^d$ )
- $\omega$  production ( $\frac{2}{3}H^u - \frac{1}{3}H^d$ )
- $\phi$  production ( $H^s, H_g$ )
- $J/\psi$  and  $\Upsilon$  production ( $H_g$ )

## Differential cross sections of vector mesons

The longitudinal and transversal differential cross sections as functions of  $|t|$  and total cross sections of heavy vector meson in photon-proton scattering as function of  $W$  and  $Q^2$  are calculated as [arXiv.2310.00980]

$$\frac{d\sigma_T}{dt} = \frac{1}{16\pi W^2(W^2 + Q^2)} [|\mathcal{M}_{++,++}|^2 + |\mathcal{M}_{+-,++}|^2], \quad (20)$$

$$\frac{d\sigma_L}{dt} = \frac{Q^2}{m_V^2} \frac{d\sigma_T}{dt}; \quad (21)$$

$$\frac{d\sigma}{dt} = \frac{d\sigma_T}{dt} + \varepsilon \frac{d\sigma_L}{dt}. \quad (22)$$

## Differential cross section of vector mesons

The gluon contribution to light vector meson electroproduction within GPD approach were calculated in [EPJC-42-281]. The helicity conservation amplitude of heavy vector meson production is given as

$$\begin{aligned} \mathcal{M}_{\mu'+, \mu+} &= \frac{e}{2} C_V \int_0^1 \frac{dx}{(x+\xi)(x-\xi+i\epsilon)} \\ &\times \left\{ \mathcal{H}_{\mu', \mu}^{V+} H_g(x, \xi, t, \mu_F) + \mathcal{H}_{\mu', \mu}^{V-} \tilde{H}_g(x, \xi, t, \mu_F) \right\}. \end{aligned} \quad (23)$$

While the helicity flip amplitude can be written as

$$\begin{aligned} \mathcal{M}_{\mu'-, \mu+} &= -\frac{e}{2} C_V \frac{\sqrt{-t}}{2m} \int_0^1 \frac{dx}{(x+\xi)(x-\xi+i\epsilon)} \\ &\times \left\{ \mathcal{H}_{\mu', \mu}^{V+} E_g(x, \xi, t, \mu_F) + \mathcal{H}_{\mu', \mu}^{V-} \tilde{E}_g(x, \xi, t, \mu_F) \right\}. \end{aligned} \quad (24)$$

Here the amplitudes  $\mathcal{H}_{\mu', \mu}^{V\pm}$  are determined as a sum and differences of amplitudes with different gluon helicities.

$$\mathcal{H}_{\mu', \mu}^{V\pm} = \left[ \mathcal{H}_{\mu'+, \mu+}^V \pm \mathcal{H}_{\mu'-, \mu-}^V \right], \quad (25)$$

## Scattering amplitudes

To calculate hard scattering amplitude we consider six gluon Feynman diagrams. After a length calculations, the hard amplitude can be cast into

$$\mathcal{H}_{\mu',\mu}^{V\pm}(x, \xi) = 64\pi^2 \alpha_s(\mu_R) \int_0^1 d\tau \int \frac{d^2\mathbf{k}_\perp}{16\pi^3} \psi(\tau, \mathbf{k}_\perp) \mathcal{F}_{\mu',\mu}^{\pm}(\tau, x, \xi, \mathbf{k}_\perp^2). \quad (26)$$

Here  $\tau$  and  $1 - \tau$  are the fraction of longitudinal part of quark (antiquark) momenta incoming to the meson wave function,  $\mathbf{k}_\perp$  is there transverse part. The  $k$ -dependent wave function of the vector meson is written as

$$\psi(\tau, \mathbf{k}_\perp) = a_v^2 f_v \exp\left(-a_v^2 \frac{\mathbf{k}_\perp^2}{\tau(1-\tau)}\right). \quad (27)$$

Here  $f_v$  is a  $J/\psi$  decay constant, the parameter  $a_v$  is fixed from the best fit  $J/\psi$  cross section and determine the average value of  $\langle \mathbf{k} \rangle_\perp^2$ .

## Hard part of scattering amplitude in $J/\psi$ production

For  $\tau = 1/2$ , the hard part of the amplitude can be written as

$$\mathcal{F}_{\mu',\mu}^{\pm} = \frac{f_{\mu',\mu}^{\pm}}{\text{denominator}} \quad (28)$$

$$\begin{aligned} \text{denominator} &= (2\mathbf{k}_{\perp}^2 + m_V^2 + Q^2)(4\xi\mathbf{k}_{\perp}^2 + (m_V^2 + Q^2)) \\ &(\xi - x) + i\epsilon)(4\xi\mathbf{k}_{\perp}^2 + (m_V^2 + Q^2)(\xi + x)) \end{aligned} \quad (29)$$

For longitudinal and transverse helicity conservation amplitudes  $f_{\mu,\mu}^+$  have a form

$$f_{00}^+ = -64\sqrt{Q^2}(m_V^2 + Q^2)^2(x^2 - \xi^2), \quad (30)$$

$$f_{11}^+ = 64m_V(m_V^2 + Q^2)^2(x^2 - \xi^2). \quad (31)$$

Here we omit  $k$  dependent terms. For the  $f_{\mu,\mu}^-$  which contains  $\tilde{H}$  contribution, we find that

$$f_{11}^- = -256(m_V^2 + Q^2)\mathbf{k}_{\perp}^2 m_V x \xi, \quad f_{00}^- = 0. \quad (32)$$

## GPDs function definitions

The GPDs are constructed adopting the double distribution representation

$$F(x, \xi, t) = \int_{-1}^1 d\beta \int_{-1+|\beta|}^{1-|\beta|} d\alpha \delta(\beta + \xi \alpha - x) f_g(\beta, \alpha, t), \quad (33)$$

$F$  with PDFs  $h$  via the double distribution functions  $f_i(\beta, \alpha, t)$ . For gluon double distribution functions, it is

$$f_g(\beta, \alpha, t) = e^{-bvt} h_i(\beta, \mu_F) \frac{15 [(1 - |\beta|)^2 - \alpha^2]^2}{16 (1 - |\beta|)^5}. \quad (34)$$

The  $t$ -dependence in PDFs  $h(\beta, \mu_F)$  is the fitted from conlinear PDF (CT18NLO, NNPDF, ABMP)

# $J/\psi$ production at different $|t|$

The  $J/\psi$  differential cross section as a function of  $W$  using GK model [arXiv.2310.00980]

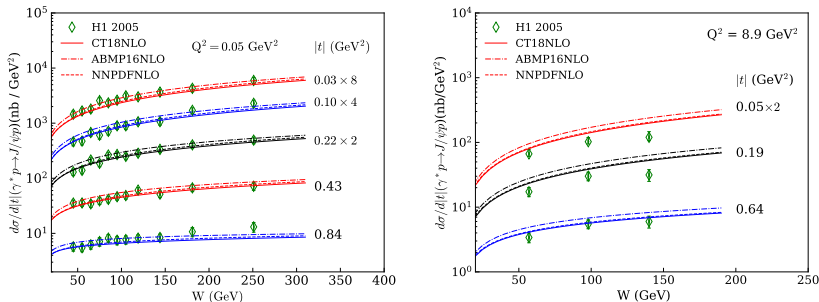


Figure 8:  $J/\psi$  differential cross section as a function of  $W$  at different  $|t|$ . The H1 experimental data are from EPJC-46-585.

- $t$ -dependencies of cross section at fix  $W$  and  $Q^2$  decrease well.
- The B-slope factor is good

# $J/\psi$ and $\Upsilon(1S)$ production in ep scattering

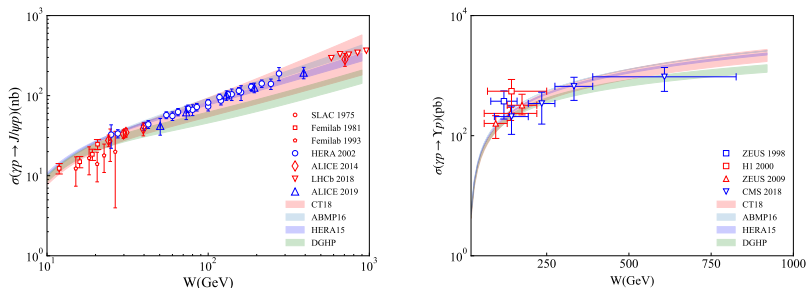


Figure 9:  $J/\psi$  and  $\Upsilon(1S)$  total cross section and at  $Q^2 = 0 \text{ GeV}^2$  vs  $W$  from low to very high energy.

- The model can describe the  $J/\psi$  photoproduction cross section at a large  $W$  region.
- Our calculation agree with the  $\Upsilon$  photoproduction cross sections.

# $J/\psi$ production at proton-proton collisions

The  $J/\psi$  differential cross section at pp collision as a function of  $W$  using GK model [arXiv. 2502.17743]

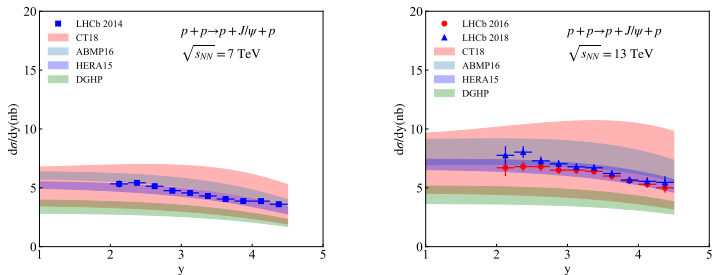


Figure 10:  $J/\psi$  production as a function of rapidity at pp UPC.

- The model can describe proton proton collision cross section at high energy.
- The cross section uncertainties of model is large since large

# $J/\psi$ production at p-Pb ultraperipheral collisions

The  $J/\psi$  rapidity distribution at p-Pb UPCs using GK model  
[arXiv.2507.20448]

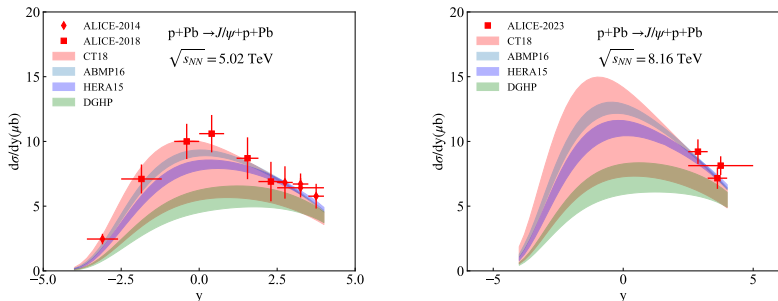


Figure 11:  $J/\psi$  production as a function of rapidity at p-Pb UPC.

- The model can describe  $J/\psi$  proton-lead collision cross section at high energy.

# Summary

We can conclude following conclusions:

- GPDs can be studied in various processes (DVCS, DDVCS, TCS, DVMP).
- GPDs method can be employed to perform heavy vector mesons production in ep scattering and UPCs.
- Gluon density can be constrained via heavy vector meson cross sections in UPCs at high energy limit.
- Results of this work can be applied in future EicC experiments to give additional essential constraints on transversity GPDs at EicC energies range.
- Important information on gluon GPDs (especially  $E_g$ ,  $H_g$ ) can be obtained at US EIC, EicC and LHCb.

*Thanks for your attentions!*